# An Optimization Reconstruction Algorithm Based on Regularization and Backtracing

Xinhe Zhang and Yufeng Liu

*Abstract*—**In compressed sensing (CS), the traditional matching pursuit algorithms have a narrow adaptability to the sparsity and a higher time complexity. To expand the adaptability to sparsity and reduce the time complexity, a regularized-subspace pursuit (R-SP) algorithm is proposed. The regularization rule of the regularized orthogonal matching pursuit (ROMP) algorithm and the backtracing mechanism of the subspace pursuit (SP) algorithm are used to improve the accuracy of atom selection. The results of experiment show that in one-dimensional signal, the reconstruction probability of each algorithm is almost the same when the sparsity *K* is small. However, when the sparsity *K* increases, the R-SP algorithm has higher reconstruction probability and obvious advantages of reconstruction time. In two-dimensional images, the reconstruction performance of R-SP algorithm is slightly worse than ROMP algorithm. What's more, the R-SP algorithm widens the range of sparsity *K*, shortens the reconstruction time and achieves the complementary advantages when compared with other algorithms.**

*Index Terms*—**Compressed sensing， matching pursuit, reconstruction algorithm, backtracing mechanism**

## I. INTRODUCTION

WITH the advent of the era of big data, the development of hardware devices cannot meet the theoretical requirements for some high-frequency signals according to Nyquist sampling theory. Under this background, compressed sensing (CS) theory emerged [1-2]. When the compressed sensing was put forward, it attracted the attention of researchers in more than half of the industrial fields. One after another, the theory of compressed sensing was applied in different fields, and the pleasing results were obtained.

Compressed sensing theory adopts a new way to collect and compress signals, which combines the high-speed sampling of original signals with compression to directly obtain the compressed data. In recent years, compressed sensing theory has been a research hotspot in the fields of image compression [3], medical imaging [4], radar imaging [5], remote sensing satellite photography [6], quantum state tomography [7], and so on, and a large number of research achievements have emerged.

Compressed sensing theory consists of three parts: signal sparse representation, observation matrix construction and reconstruction algorithm. Compressed sensing is aimed at sparse signal, but most signals in nature are not sparse. Therefore the signal should be sparsely processed by multiplying a sparse matrix; it makes the signal is sparse in another transform domain. The transformation methods include discrete cosine transform (DCT), discrete Fourier transform (DFT), wavelet transform (WT), and so on [8-9]. The number of rows of observation matrix should be less than the number of columns. The compressed signal is obtained by multiplying the observation matrix with the sparse signal. Unfortunately, the design of observation matrix is very difficult. Many studies have shown that Gaussian matrix and partial Hadamard matrix can be used as observation matrix. At the receiver side, the compressed signal needs to be reconstructed, and the reconstruction algorithm is of great significance to the reconstruction of the compressed signal.

The research on the signal reconstruction has been a hot spot in this field. After more than ten years of research and development, the reconstruction algorithm can be divided into three categories: greedy algorithm, convex optimization algorithm, and combined algorithm [10]. The convex optimization algorithm is based on $\ell_1$ norm to solve an approximation solution of a convex optimization problem, such as interior point method [11], iterative hard threshold algorithm [12] and FOCUSS algorithm [13]. The greedy algorithm is to find the approximate solution by solving the $\ell_0$ norm, and solves the original signal by means of sparse approximation, such as orthogonal matching pursuit (OMP) algorithm [14], regularized orthogonal matching pursuit (ROMP) algorithm [15], subspace pursuit (SP) algorithm [16], compressive sampling matching pursuit (CoSaMP) algorithm [17], and so on. The combined algorithm, such as Fourier sampling algorithm [18], has a relatively good reconstruction performance. However, due to various constraints and strict requirements on the system, it cannot be widely applied in the compressed sensing theory.

Greedy algorithm is widely used because of its high precision and fast running speed. Many studies have shown that the traditional matching pursuit algorithm relies on the sparsity $K$, which is far less than the observation dimension $M$. If the signal sparsity does not meet the requirements of the algorithm, the reconstruction accuracy is greatly reduced. Therefore, it is of great significance to expand the adaptability to sparsity $K$. In this paper, the regularized-subspace pursuit (R-SP) algorithm combining the ROMP algorithm and SP

Manuscript received December 15, 2020; revised March 30, 2021. This work was supported in part by the Excellent Talents Training Program of University of Science and Technology Liaoning (Grant No. 2017RC10) and the Doctoral Scientific Research Foundation of Liaoning Province (Grant No. 2020-BS-225).

Xinhe Zhang is an Associate Professor of School of Electronic and Information Engineering, University of Science and Technology Liaoning, Anshan, 114051 China. (corresponding author, phone: 86-412-5929725; email: 527075114@qq.com, xhzhang@ustl.edu.cn).

Yufeng Liu is a Postgraduate of School of Electronic and Information Engineering, University of Science and Technology Liaoning, Anshan, 114051 China. (email: 892824208@qq.com).

algorithm is proposed. Simulation experiments on one-dimensional signal and two-dimensional image are carried out to evaluate the reconstruction probability, average run time and peak signal to noise ratio (PSNR) parameters.

The following are the novel contributions of this paper:

1) The R-SP algorithm proposed in this paper combines the ROMP algorithm and SP algorithm in greedy algorithm. And the adaptability of R-SP algorithm to sparsity $K$ has exceeded that of SP and ROMP algorithms.

2) In one-dimensional signal reconstruction, the reconstruction probability of the proposed R-SP algorithm is higher than other algorithms. In two-dimensional image reconstruction, R-SP algorithm obtains the time advantage and reconstruction accuracy of ROMP algorithm, and the adaptability to sparsity $K$ of SP algorithm.

*Notation*: Boldface uppercase/lowercase letters represent the matrices and vectors, respectively. $|\bullet|$ represents the magnitude of a complex quantity or the cardinality of a given set. $\|\bullet\|_0$ and $\|\bullet\|_1$ represent the zero- and one-norm of a vector, respectively. $\mathbb{R}$ stands for the field of real numbers. $(\bullet)^T$ represents the transpose of a vector or matrix.

## II. Compressed sensing

Consider a real-valued, finite-length, one-dimensional, discrete-time signal $\boldsymbol{x} \in \mathbb{R}^N$. We say that the signal $\boldsymbol{x}$ is $K$-sparse when it has at most $K$ nonzero, i.e., $\|\boldsymbol{x}\|_0 \le K$, where $\|\boldsymbol{x}\|_0 = \#\left(i \middle| x_i \ne 0\right)$, that is a total number of non-zero elements in a vector. Give a signal $\boldsymbol{x} \in \mathbb{R}^N$, we consider measurement systems that acquires $M$ linear measurements. We can represent the system mathematically as

$$\boldsymbol{y} = \boldsymbol{\Phi x}, \tag{1}$$

where $\boldsymbol{y} \in \mathbb{R}^M$ is the observation vector and $\boldsymbol{\Phi} \in \mathbb{R}^{M \times N}$ is the observation matrix, respectively. Generally, $M$ is much smaller than $N$. The observation matrix $\boldsymbol{\Phi}$ must allow the reconstruction of signal $\boldsymbol{x}$ from $M$ measurements. A necessary and sufficient condition is that, the observation matrix $\boldsymbol{\Phi}$ should meet the restricted isometry property (RIP) [19]:

$$(1-\delta)\|\boldsymbol{x}\|_2^2 \le \|\boldsymbol{\Phi x}\|_2^2 \le (1+\delta)\|\boldsymbol{x}\|_2^2, \tag{2}$$

where $\delta \in (0,1)$. The RIP property states the one-to-one mapping relationship between the original space and the sparse space. That is, the signal $\boldsymbol{x}$ can be reconstructed and the uniqueness is guaranteed.

We are concerned with the problem of the recovery of the unknown signal $\boldsymbol{x}$ from the observation signal $\boldsymbol{y}$. (1) can be formulated into an $\ell_0$-norm minimization problem, which seeks a solution to the problem:

$$\begin{aligned} &\hat{\boldsymbol{x}} = \arg\min_{\boldsymbol{x}} \|\boldsymbol{x}\|_0 \\ &s.t. \quad \boldsymbol{y} = \boldsymbol{\Phi x} \end{aligned}. \tag{3}$$

Since the object function $\|\bullet\|_0$ is non-convex, (3) is potentially difficult to solve. One avenue for translating this problem into something more tractable is to replace $\|\bullet\|_0$ with its convex approximation $\|\bullet\|_1$. Specifically, we consider

$$\begin{aligned} &\hat{\boldsymbol{x}} = \arg\min_{\boldsymbol{x}} \|\boldsymbol{x}\|_1 \\ &s.t. \quad \boldsymbol{y} = \boldsymbol{\Phi x} \end{aligned}, \tag{4}$$

where $\|\boldsymbol{x}\|_1 = \sum_{i=1}^{N} |x_i|$ is the $\ell_1$-norm of the vector $\boldsymbol{x}$.

The main advantage of the $\ell_1$-norm minimization is that it is a convex optimization problem that can be solved efficiently by linear programming techniques.

Specially, when greedy algorithms are used to solve (3), the reconstruction accuracy will be slightly reduced and the corresponding reconstruction time will be significantly shortened, which is more widely applied than other algorithms [20].

## III. The Proposed R-SP Algorithm

The OMP algorithm, a sequential selection method, only selects the most relevant atom in the process of atom selection. It is shown that the signal recovery performance of OMP algorithm is good when the correlations between any two columns of the observation matrix are small. Its symbol error rate curve exhibits a flooring tendency even at moderate signal to noise ratio. In each iteration, OMP identifies the index which has maximum absolute correlation with the current residual. Only one atom is selected in each iteration, and it takes multiple iterations to recover original signal. ROMP algorithm has a fast speed, but it has a narrow adaptability to the sparsity $K$. Under the same sparsity $K$, to accurately recover the original signal $\boldsymbol{x}$, the observation dimension $M$ must be greater than that of OMP, SP and other algorithms. When the observation dimension $M$ is the same, ROMP algorithm has higher requirements to sparsity $K$, which is far less than the observation dimension $M$. Moreover, the backtracing mechanism used in SP algorithm increases the accuracy of atom selection. Compared with ROMP algorithm, SP algorithm has expanded the adaptive range of sparsity $K$. Based on the shortcomings of the above algorithms, an R-SP algorithm combining ROMP algorithm and SP algorithm is proposed in this paper. In the first stage, ROMP algorithm is used to select partial atoms. When the number of selected atoms meets the requirements, the second stage is entered. In the second stage SP algorithm is adopted to recover the signal. The number of atoms selected in the first stage is added to the number of atoms selected by SP algorithm, and then the backtracing mechanism is utilized to improve the reconstruction performance. The precision of atom selection in the first stage and the backtracing mechanism in the second stage provide double insurance for atom selection, which improve the precision of atom selection of the R-SP algorithm.

The main steps of R-SP algorithm are summarized below.

**Input**: Observation matrix $\boldsymbol{\Phi} \in \mathbb{R}^{M \times N}$, observation vector $\boldsymbol{y} \in \mathbb{R}^N$, signal sparsity $K$.

**Output**: The estimated signal $\hat{\boldsymbol{x}}$.

**The first stage:**

1) Initialization the residual $\boldsymbol{r}_0^{(1)} = \boldsymbol{y}$, the index set $\Lambda_0^{(1)} = \varnothing$, the atom set $\boldsymbol{\Phi}_{\Lambda_0^{(1)}} = \varnothing$, where $\varnothing$ represents empty set, the iteration counter $t = 1$.

2) Calculate the correlation coefficient between residual $\boldsymbol{r}_{t-1}^{(1)}$ and observation matrix $\boldsymbol{\Phi}$, i.e., $\boldsymbol{u} = \left|\boldsymbol{\Phi}^T \boldsymbol{r}_{t-1}^{(1)}\right|$, and choose a set $J$ of $K$ biggest coordinates or all of its nonzero coordinates in $\boldsymbol{u}$ (if the number of nonzero value is less than $K$).

3) Regularize: Among all subsets $J_0 \subset J$ with comparable coordinates $|\boldsymbol{u}(i)| \le 2|\boldsymbol{u}(j)|$ ($i, j \in J_0$), choose subset $J_0$ with the maximum energy including the largest correlation coefficient.

4) Augment the index set and the matrix of chosen atoms: $\Lambda_t^{(1)} = \Lambda_{t-1}^{(1)} \cup J_0$ and $\boldsymbol{\Phi}_{\Lambda_t}^{(1)} = \left[\boldsymbol{\Phi}_{\Lambda_{t-1}}^{(1)}, \boldsymbol{\Phi}_{J_0}\right]$.

5) Solve a least squares problem of $\boldsymbol{y} = \boldsymbol{\Phi}_{\Lambda_t}^{(1)} \boldsymbol{x}_t^{(1)}$ to obtain a approximate solution: $\hat{\boldsymbol{x}}_t^{(1)} = \arg\min_{\boldsymbol{x}_t^{(1)}} \left\|\boldsymbol{y} - \boldsymbol{\Phi}_{\Lambda_t}^{(1)} \boldsymbol{x}_t^{(1)}\right\|_2$.

6) Calculate the residual $\boldsymbol{r}_t^{(1)} = \boldsymbol{y} - \boldsymbol{\Phi}_{\Lambda_t}^{(1)} \hat{\boldsymbol{x}}_t^{(1)}$.

7) If $\|\Lambda_t\|_0 > ceil(K/2)$, go to step 8). Increment $t$, if $t \le K$ go to step 2); else go to step 8).

**The second stage:**

8) Initialization the residual $\boldsymbol{r}_0^{(2)} = \boldsymbol{r}_t^{(1)}$, the index set $\Lambda_0^{(2)} = \Lambda_t^{(1)}$, the atom set $\boldsymbol{\Phi}_{\Lambda_0}^{(2)} = \boldsymbol{\Phi}_{\Lambda_t}^{(1)}$, and the iteration counter $i = 1$.

9) Calculate the correlation coefficient between residual $\boldsymbol{r}_{i-1}^{(2)}$ and observation matrix $\boldsymbol{\Phi}$, i.e., $\boldsymbol{u} = \left|\boldsymbol{\Phi}^T \boldsymbol{r}_{i-1}^{(2)}\right|$, and choose a set $L_0$ of $K$ biggest coordinates or all of its nonzero coordinates in $\boldsymbol{u}$ (if the number of nonzero value is less than $K$).

10) Augment the index set $\Lambda_i^{(2)} = \Lambda_{i-1}^{(2)} \cup L_0$.

11) If the length of $\Lambda_i^{(2)}$ is greater than the observation dimension $M$, then $\hat{\boldsymbol{x}} = 0$, and go to step 16); otherwise augment the matrix of chosen atoms $\boldsymbol{\Phi}_{\Lambda_i}^{(2)} = \left[\boldsymbol{\Phi}_{\Lambda_{i-1}}^{(2)}, \boldsymbol{\Phi}_{L_0}\right]$.

12) Solve a least squares problem of $\boldsymbol{y} = \boldsymbol{\Phi}_{\Lambda_i}^{(2)} \boldsymbol{x}_i^{(2)}$ obtain a new signal estimation: $\hat{\boldsymbol{x}}_i^{(2)} = \arg\min_{\boldsymbol{x}_i^{(2)}} \left\|\boldsymbol{y} - \boldsymbol{\Phi}_{\Lambda_i}^{(2)} \boldsymbol{x}_i^{(2)}\right\|_2$.

13) Obtain the signal $\hat{\boldsymbol{x}}_{iK}^{(2)}$ from the $K$ maximum elements of $\hat{\boldsymbol{x}}_i^{(2)}$, the corresponding index set $\Lambda_{iK}^{(2)}$ and atom set $\boldsymbol{\Phi}_{iK}^{(2)}$; and update the index set $\Lambda_i^{(2)} = \Lambda_{iK}^{(2)}$.

14) Update the residual: $\boldsymbol{r}_i^{(2)} = \boldsymbol{y} - \boldsymbol{\Phi}_{iK}^{(2)} \hat{\boldsymbol{x}}_{iK}^{(2)}$.

15) If $i \le K$, then $i = i + 1$, go to step 9); if $i > K$ or residual $\boldsymbol{r}_i^{(2)} = 0$, quit the iteration and go to step 16).

16) Obtain the estimated signal $\hat{\boldsymbol{x}}$.

## IV. Simulation

To verify that the R-SP algorithm proposed in this paper improves the adaptability to sparsity $K$ and reduce the run time, a series of simulation experiments are carried out. The experimental environment is CPU Core i5-5200U, main frequency is 2.20GHz, the memory is 4GB, and the simulation software is MATLAB R2016a.

### A. One-Dimensional Signal Reconstruction Experiments

**Experiment 1**: The reconstruction probability is compared under the condition of fixed $K$ and varying $M$.

The random signal with length of 256 is generated randomly, and the observation matrix $\boldsymbol{\Phi}$ is $M \times N$ Gaussian matrix. When the error between the reconstructed signal $\hat{\boldsymbol{x}}$ and the original signal $\boldsymbol{x}$ is less than $10^{-6}$, we consider that the original signal has been reconstructed successfully. The reconstruction probability is the percentage ratio of the number of successful reconstructions to the number of experiments. When the sparsity $K$ is 25 and 40, the reconstruction probability curves are shown in Fig. 1 and Fig. 2, respectively.

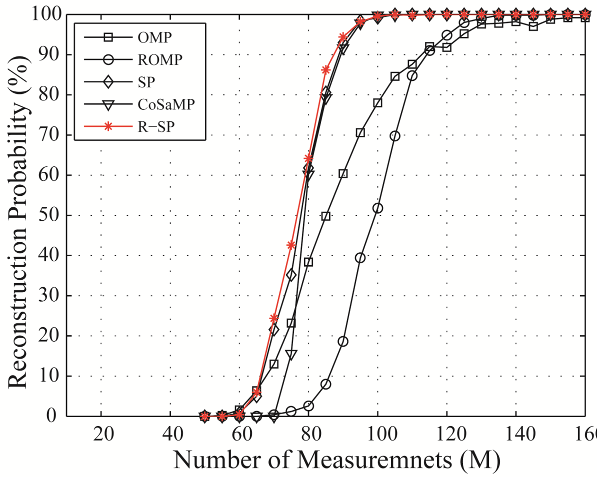


Fig. 1. Simulation curves of reconstruction probability versus the number of measurements when sparsity $K$=25.

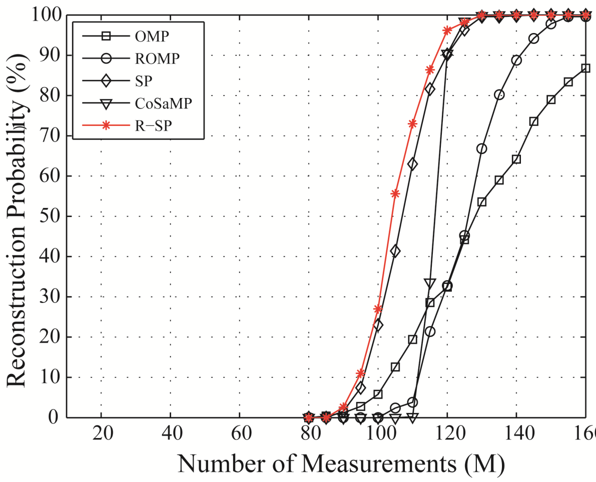


Fig. 2. Simulation curves of reconstruction probability versus the number of measurements when sparsity $K$=40.

It can be seen from Fig. 1 and Fig. 2 that when the sparsity $K$ is small, the reconstruction probability is basically the same except ROMP algorithm. With the increase of sparsity $K$, the reconstruction probability of R-SP algorithm is higher than that of other algorithms in the condition of the same observation dimension $M$.

**Experiment 2**: The reconstruction probability experiment is conducted under the condition of fixed $M$ and varying $K$.

The random signal with length of 256 is generated randomly, the sparsity $K$ is ranged from 10 to $\frac{4}{5}M$, and the observation matrix $\boldsymbol{\Phi}$ is $M \times N$ Gaussian matrix. When the observation dimension $M$ is equal to 128 and 160, and reconstruction probability curves are shown in Fig. 3 and Fig. 4, respectively.

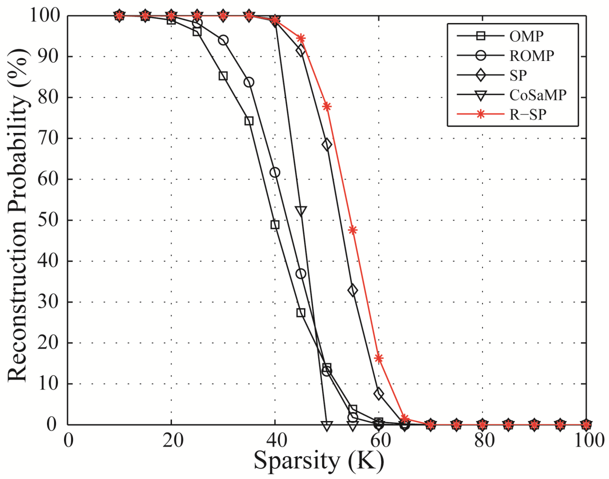


Fig. 3. Simulation curves of reconstruction probability versus sparsity $K$ when observation dimension $M = 128$.

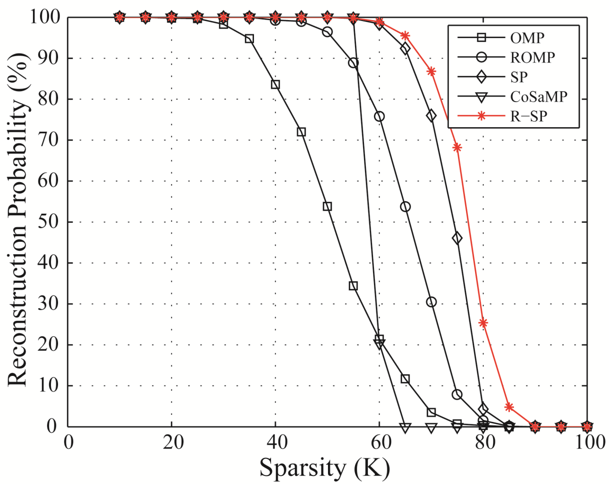


Fig. 4. Simulation curves of reconstruction probability versus sparsity $K$ when observation dimension $M = 160$.

We can conclude from the simulation curves in Fig. 3 and Fig. 4 that when the observation dimension $M$ is the same, the reconstruction probability decreases with the increase of sparsity $K$. Compared with other algorithms, the R-SP algorithm proposed in this paper still has a high reconstruction probability in the case of bigger sparsity $K$, which improves the applicable range.

**Experiment 3**: The average run time of different algorithms is compared in this experiment. The random signal with length of 256 is generated randomly, the observation dimension $M$ is 128, and the sparsity $K$ is ranged from 5 to 45, and the observation matrix $\boldsymbol{\Phi}$ is $M \times N$ Gaussian matrix. The average run time simulation curves are shown in Fig. 5.

It can be seen from Fig. 5 that the run time of the proposed R-SP algorithm is almost the same to that of the other algorithms when the sparsity $K$ is small. With the increase of sparsity $K$, the run time of all the algorithms increases. In all above-mentioned algorithms, the run time of CoSaMP algorithm increases rapidly, and the ROMP algorithm runs the fastest. When the sparsity $K$ is greater than 40, the R-SP algorithm has the obvious advantage over SP, OMP, and CoSaMP algorithms.

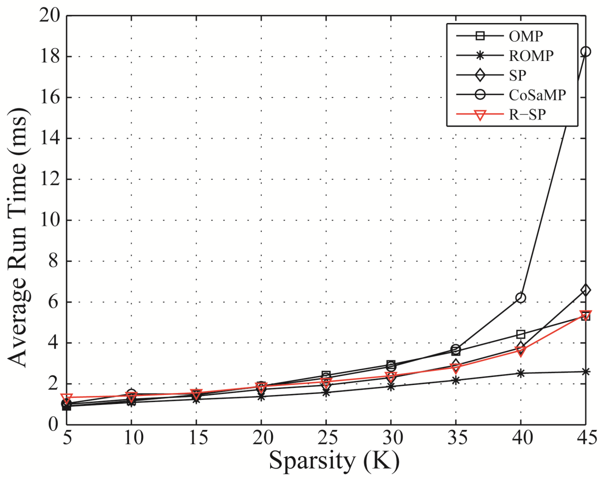


Fig. 5. Simulation curves of average run time versus sparsity $K$.

From the above experimental curves Fig.1 – Fig. 6, we can conclude that the R-SP algorithm combines the time superiority of ROMP algorithm with the reconstruction accuracy of SP algorithm. That is, the R-SP algorithm outperforms the performance of ROMP and SP algorithms.

### B. *Two-Dimensional Image Reconstruction Experiments*

**Experiment 4**: Lena image with $256 \times 256$ pixels is used in this experiment. The observation matrix $\boldsymbol{\Phi}$ is an $M \times N$ Gaussian matrix. Since the image is a non-sparse signal, the image must be sparsely processed by multiplying a $N \times N$ wavelet transform matrix. We assume that the sparsity $K$ is 30. In the same experimental conditions, OMP, ROMP, SP, CoSaMP and the R-SP algorithm proposed in this paper are compared. The parameter peak signal-to-noise (PSNR) is used to evaluate the reconstructed performance. The PSNR comparison results of different algorithms are listed in TABLE I.

TABLE I
PSNR Comparison of Different Algorithms (unit: dB)

| M/N | OMP | ROMP | SP | CoSaMP | R-SP |
|---|---|---|---|---|---|
| 0.5 | 26.51 | 27.32 | 27.27 | 26.73 | 27.42 |
| 0.6 | 27.76 | 29.57 | 28.73 | 28.81 | 28.76 |
| 0.7 | 28.55 | 30.74 | 29.50 | 29.71 | 29.52 |
| 0.8 | 29.10 | 31.97 | 29.93 | 30.14 | 29.96 |

According to TABLE I, when the compression ratio is 0.5, there is little different in the PSNR of each reconstruction algorithm. With the increase of compression ratio, the PSNR of all algorithms increases. Among them, the PSNR value of ROMP algorithm increases fastest and the reconstruction quality is the best. The PSNR values of R-SP, SP and CoSaMP algorithms are almost the same, and the reconstruction quality is slightly worse. The PSNR of OMP algorithm increases slowly, and reconstruction quality is the worst.

**Experiment 5**: To illustrate the advantages of the proposed R-SP algorithm, the influence of different sparsity $K$ on the reconstruction performance is studied. Lena image with $256\times 256$ pixels is used in the experiment. The observation matrix $\boldsymbol{\Phi}$ is $M\times N$ Gaussian matrix, and the sparse matrix is $N\times N$ wavelet transform matrix. The sparsity $K$ is ranged from 30 to 65, and the PSNR and reconstruction time under different sparsity $K$ are compared. OMP, ROMP, SP, CoSaMP and R-SP algorithms proposed in this paper are compared under the same experimental conditions. The PSNR and reconstruction time of all above-mentioned algorithms under different sparsity $K$ are listed in TABLE II and TABLE III, respectively.

TABLE II
PSNR COMPARISON OF ALGORITHMS UNDER DIFFERENT SPARSITY

| $K$ | OMP | ROMP | SP | CoSaMP | R-SP |
|---|---|---|---|---|---|
| 30 | 26.50 | 27.27 | 27.27 | 26.73 | 27.42 |
| 35 | 26.61 | 27.28 | 26.89 | 26.12 | 27.50 |
| 40 | 26.63 | 27.21 | 26.62 | 25.26 | 27.24 |
| 45 | 26.70 | 26.99 | 26.33 | 18.48 | 27.46 |
| 50 | 26.84 | 25.66 | 25.15 | 11.66 | 25.88 |
| 55 | 26.85 | 25.51 | 23.32 | 12.83 | 25.95 |
| 60 | 26.43 | 20.99 | 22.97 | 14.81 | 24.83 |
| 65 | 26.72 | 20.84 | 12.77 | 7.24 | 24.06 |

TABLE III
RECONSTRUCTION TIME OF ALGORITHMS UNDER DIFFERENT SPARSITY
(UNIT: S)

| $K$ | OMP | ROMP | SP | CoSaMP | R-SP |
|---|---|---|---|---|---|
| 30 | 1.1723 | 0.4227 | 4.3478 | 6.5039 | 4.1881 |
| 35 | 1.5634 | 0.5212 | 6.0710 | 8.6890 | 6.2680 |
| 40 | 1.9850 | 0.5766 | 7.7060 | 11.9484 | 7.8870 |
| 45 | 2.2056 | 0.6916 | 9.7147 | 12.8017 | 9.9858 |
| 50 | 2.6532 | 0.8189 | 13.3665 | 0.3625 | 12.1869 |
| 55 | 3.0784 | 0.8674 | 15.5423 | 0.3733 | 14.6208 |
| 60 | 3.5987 | 0.8592 | 18.0144 | 0.3815 | 15.8059 |
| 65 | 4.0994 | 0.8566 | 0.2452 | 0.0475 | 6.8765 |

As can be seen from TABLE II, OMP and R-SP algorithms have a wide adaptability to sparsity $K$, and can reconstruct the image more accurately when the sparsity is large. While ROMP and SP algorithms have a narrow adaptability to the sparsity $K$. With the increase of the sparsity $K$, the reconstruction performance will decline and recovery probability will be reduced. When sparsity $K$ exceeds 60, ROMP and SP algorithms cannot reconstruct the signal accurately. CoSaMP has the worst adaptability to sparsity $K$, and the image cannot be reconstructed when the sparsity $K$ is larger than 40. Compared with SP and ROMP algorithms, the proposed R-SP algorithm expands the adaptability to sparsity $K$.

We can conclude from TABLE III, the reconstruction time of R-SP algorithm has obvious advantages over SP algorithm. Considering TABLE II and TABLE III, we can conclude that R-SP algorithm obtains the time advantage and reconstruction accuracy of ROMP algorithm, and combines the adaptability of SP algorithm to sparsity $K$. Compared with ROMP and SP algorithms, R-SP algorithm proposed in this paper achieves a better reconstruction performance.

## V. CONCLUSION

In this paper, R-SP algorithm is proposed. In the first stage, partial atoms are selected by using the atoms selection rule of ROMP algorithm. In the second stage, SP algorithm is adopted to increase the accuracy of selected atoms by using the backtracing mechanism. Base on the simulation curves, the adaptability of R-SP algorithm to sparsity exceeds that of OMP, ROMP, SP and CoSaMP algorithms. Except ROMP algorithm, R-SP algorithm has obvious advantages in reconstruction time. The combination of ROMP algorithm and SP algorithm achieves a better reconstruction performance.

## REFERENCES

[1] Y. C. Eldar, and G. Kutyniok, *Compressed sensing: theory and applications*. Cambridge: Cambridge University Press, 2012, ch. 2.

[2] D. L. Donoho, "Compressed sensing", *IEEE Transactions on Information Theory*, vol. 52, no. 4, pp. 1289-1306, Apr. 2006.

[3] Y. S. Liu, Z. F. Zhan, J. F. Cai, D. Guo, Z. Chen, and X. B. Qu, "Projected iterative soft-thresholding algorithm for tight frames in compressed sensing magnetic resonance imaging," *IEEE Transactions on Medical Imaging*, vol. 35, no. 9, pp. 2130-2140, Sep. 2016.

[4] S. Datta, and B. Deka, "Efficient interpolated compressed sensing reconstruction scheme for 3D MRI," *IET Image Processing*, vol. 12, no. 11, pp. 2119-2127, Nov. 2018.

[5] L. Zhang, M. D. Xing, C. W. Qiu, J. Li, and Z. Bao, "Achieving higher resolution ISAR imaging with limited pulses via compressed sampling," *IEEE Geoscience and Remote Sensing Letters*, vol. 6, no. 3, pp.567-571, Mar. 2009.

[6] M. T. Alonso, P. Lopez-Dekker, and J. J. Mallorqui, "A novel strategy for radar imaging based on compressive sensing," *IEEE Transactions on Geoscience and Remote Sensing*, vol. 48, no. 12, pp. 4285-4295, Dec. 2011.

[7] J. Yang, S. Cong, and S. Kuang, "Real-time quantum state estimation based on continuous weak measurement and compressed sensing," Lecture Notes in Engineering and Computer Science: Proceedings of the International MultiConference of Engineers and Computer Scientists 2018, 14-16 March, 2018, Hong Kong, pp. 499-504.

[8] R. Karim, S. Pervin, U. M. Ima, and M. Khaliluzzaman, "Study on performance analysis of HQAM for DCT and DWT based compressed image transmission over AWGN channel," *International Journal of Computer Science Issues*, vol. 12, no. 3, pp. 96-102, Mar. 2017.

[9] X. Wang, and W. Fang, "Deterministic construction of compressed sensing matrices from codes," *International Journal of Foundations of Computer Science*, vol. 28, no. 2, pp. 99-109, Feb. 2017.

[10] H. Tsutsu, and Y. Morikawa, "An $l_p$ norm minimization using auxiliary function for compressed sensing," Lecture Notes in Engineering and Computer Science: Proceedings of the International MultiConference of Engineers and Computer Scientists 2012, March 14-16, 2012, Hong Kong, pp. 70-77.

[11] S. J. Kim, K. Koh, M. Lustig, S. Boyd, and D. Gorinevsky, "An interior-point method for large-scale $l_1$-regularized least squares," *IEEE Journal of Selected Topics in Signal Processing*, vol. 8, no. 3, 1519-1555, Mar. 2007.

[12] D. Ingrid, M. Defrise, and C. D. Mol, "An iterative thresholding algorithm for linear inverse problems with a sparsity constraint," *Communications on Pure and Applied Mathematics*, vol. 57, no. 11, pp. 1413- 1457, Nov. 2004.

[13] I. F. Gorodnitski, and B. D. Rao, "Sparse signal reconstruction from limited data using FOCUSS: a reweighted norm minimization algorithm," *IEEE Transactions on Signal Processing*, vol. 45, no. 3, pp. 600-616, Mar. 1997.

[14] J. A. Tropp, and A. C. Gilbert, "Signal recovery from random measurements via orthogonal matching pursuit," *IEEE Transactions on Information Theory*, vol. 53, no. 12, pp. 4655-4666, Dec. 2007.

[15] D. Needell, and R. Vershynin, "Uniform uncertainty principle and signal recovery via regularized orthogonal matching pursuit,"

*Foundations of Computational Mathematics*, vol. 9, no. 3, pp. 317-334, Mar. 2009.
[16] W. Dai, and O. Milenkovic, "Subspace pursuit for compressive sensing signal reconstruction," *IEEE Transactions on Information Theory*, vol. 55, no. 5, pp. 2230- 2248, May 2009.
[17] D. Needell, and J. A. Tropp, "CoSaMP: Iterative signal recovery from incomplete and inaccurate samples," *Applied and Computational Harmonic Analysis*, vol. 26, no. 3, pp. 301-321, Mar. 2009.
[18] A. C. Gilbert, S. Muthukrishnan, and M. J. Strauss, "Improved time bounds for near-optimal sparse Fourier representations," in *Proceedings of SPIE-The International Society for Optical Engineering*, 2004, pp. 398-412.
[19] E. J. Candes, and T. Tao, "Decoding by linear programming," *IEEE Transaction on Information Theory*, vol. 51, no. 12, pp. 4203-4215, Dec. 2005.
[20] M. M. Shi, "Research of matching pursuit reconstruction algorithms based on compressive sensing," M. S. thesis, Nanjing University of Posts and Telecommunications, Nanjing, P. R. China, 2018.

**XINHE Zhang** was born in Hebei Province, P. R. China, received the B.S. degree in Application of Electronic Technology from Anshan Iron and Steel Technology, Anshan, P. R. China, the M.S. degree in Control Theory and Control Engineering from Anshan University of Science and Technology, Anshan, P. R. China, the Ph.D. degree in Communication and Information Systems from Dalian University of Technology, Dalian, P. R. China, in 2002, 2005, 2017. His research interests include signal processing and compressed sensing.

**YUFENG LIU** was born in Hebei Province, P. R. China, received the B.S. degree in Electrical Engineering and Automation from Yantai Nanshan College, Yantai, P. R. China, in 2018.

He is currently pursuing the M.S. degree in Control Engineering with University of Science and Technology Liaoning, Anshan, P. R. China. His research interest is compressed sensing and its applications.